

Cite this: *Chem. Sci.*, 2025, 16, 139

All publication charges for this article have been paid for by the Royal Society of Chemistry

P⁺ addition and transfer involving a tetraphosphenium ion†

Roman Franz,^a Máté Bartek,^b Clemens Bruhn,^a Zsolt Kelemen^b and Rudolf Pietschnig^b ^{*,a}

Triphospha[3]ferrocenophane Fe(C₅H₄-PTip)₂PCl (Tip = 2,4,6-tri(isopropyl)phenyl) has been prepared and its suitability to generate the corresponding bisphosphanylphosphenium ion has been explored. By formal addition of P⁺ to the latter, an unprecedented tetraphosphenium ion forms which likewise is capable of P⁺ transfer and qualifies as Lewis superacid based on its computed fluoride ion affinity. As a solid, this species is stable and conveniently storable, featuring a remarkably long P–P bond (2.335(5) Å). From this tetraphosphenium ion, known and unprecedented triphosphenium ions have been generated *via* P⁺ transfer in solution, including a triphosphenium ion with P–H functionalities. Moreover, the latter has been obtained by tautomeric rearrangement from the corresponding hydrophosphane precursor. The bonding situation and details of the P⁺ transfer have been investigated by DFT calculations and experimental methods like multinuclear NMR spectroscopy and SC-XRD.

Received 8th October 2024
Accepted 25th November 2024

DOI: 10.1039/d4sc06823h

rsc.li/chemical-science

Introduction

The transfer of single phosphorus atoms has emerged as a hot topic in recent years with a special focus on P(0) or P[−] fragments.^{1–14} By contrast, P⁺ ion transfer is far less explored,^{15–23} and in addition needs to be distinguished from the transfer of substituted P(i) fragments with more than one atom, such as phosphinidenes. So called triphosphenium ions are established reagents for the transfer of formally unsubstituted P⁺ and have been carefully studied by Macdonald and co-workers in recent years.^{15–24} The first triphosphenium ions have been reported by Schmidpeter *et al.* in the 1980s as the first isolable P(i) compound in which the formal charge of P⁺ is also preserved as a net charge.^{25,26} It needs to be pointed out that – despite their similar name – the above mentioned triphosphenium ions are only distantly related to actual phosphonium ions [PR₂]⁺ with the latter featuring an electron sextet, in contrast to triphosphenium ions with an electron octet at the central phosphorus atom (Fig. 1).²⁷ Phosphenium ions are valence isoelectronic and isolobal to neutral carbene analogues such as

[ER₂] (E = C, Si, Ge, Sn, Pb).^{28,29} In addition, the positive charge imparts pronounced electrophilic character to phosphonium ions, comparable to Lewis acidic carbenium or silicenium ions [R₃E]⁺ (E = C, Si) which in turn lack an electron lone pair, however.³⁰ Consequently, phosphonium ions are highly reactive species which, for a long time, could only be detected in the gas phase until the development of thermodynamically stabilized examples,^{31–42} with the term NHP being in use for N-heterocyclic phosphonium ions of the type I⁺ (Fig. 1) in analogy to isolobal NHCs.^{40,43–46}

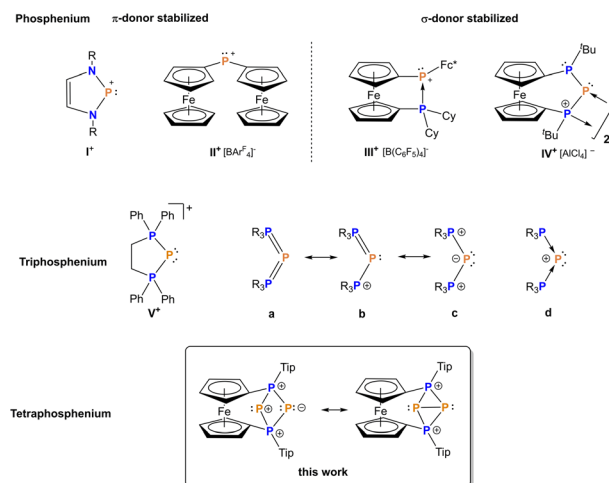


Fig. 1 Comparison of phosphonium ions I⁺, II⁺,⁵⁰ III⁺,⁴² and IV⁺,⁵⁴ (top) to triphosphenium ions V⁺ (middle) and a tetraphosphenium ion (bottom).

^aInstitute for Chemistry, CINSaT, University of Kassel, Heinrich-Plett-Straße 40, 34132 Kassel, Germany. E-mail: pietschnig@uni-kassel.de; Web: <https://www.uni-kassel.de/go/hybrid>

^bDepartment of Inorganic and Analytical Chemistry, Budapest University of Technology and Economics, Műegyetem Rkp 3, 1111 Budapest, Hungary. E-mail: kelemen.zsolt@vbk.bme.hu

† Electronic supplementary information (ESI) available: The synthesis and characterization of the compounds, experimental procedures, SCXRD details, molecular structure of 2 in the solid state, computational details, NMR spectra. CCDC 2328571–2328573. For ESI and crystallographic data in CIF or other electronic format see DOI: <https://doi.org/10.1039/d4sc06823h>

Thermodynamic stabilization has been achieved for carbon substituted (nitrogen-free) phosphonium ions as well, using ylidic^{47,48} or electron-rich olefinic carbon atoms,⁴⁹ or ferrocenyl substituted phosphonium ions such as **II**⁺ and **III**⁺ (Fig. 1).^{42,50–52} Moreover, Beckmann *et al.* succeeded in isolating a kinetically stabilized phosphonium ion recently.⁵³ For increased reactivity, *in situ*-formed, non-stabilized phosphonium ions have been employed as versatile reaction partners to construct polyphosphorus compounds, activate small molecules and alkenes.^{34,54–61} In line with this, bisphosphanylphosphonium ions **IV**⁺, which could be referred to as P-heterocyclic phosphonium ions (PHPs) in analogy to the above mentioned NHPs, feature insufficient stabilization by adjacent phosphanyl units and consequently undergo either dimerization or fragmentation^{54,62} involving P–C bond activation, with the P₃-unit remaining intact (Fig. 1).^{54,62}

Using an *in situ* generated bisphosphanylphosphonium ion equipped with a suitable substitution pattern, we report here the first transfer of formally monoatomic P⁺ to a phosphonium cation, resulting in the formation of a characteristic tetraphosphorus dication which we refer to as tetraphosphonium ion. This contrasts other known examples of P⁺ transfer proceeding to nucleophilic substrates such as amines, phosphanes, NHCs or carbonylmetallates to name just a few.^{15–17,63}

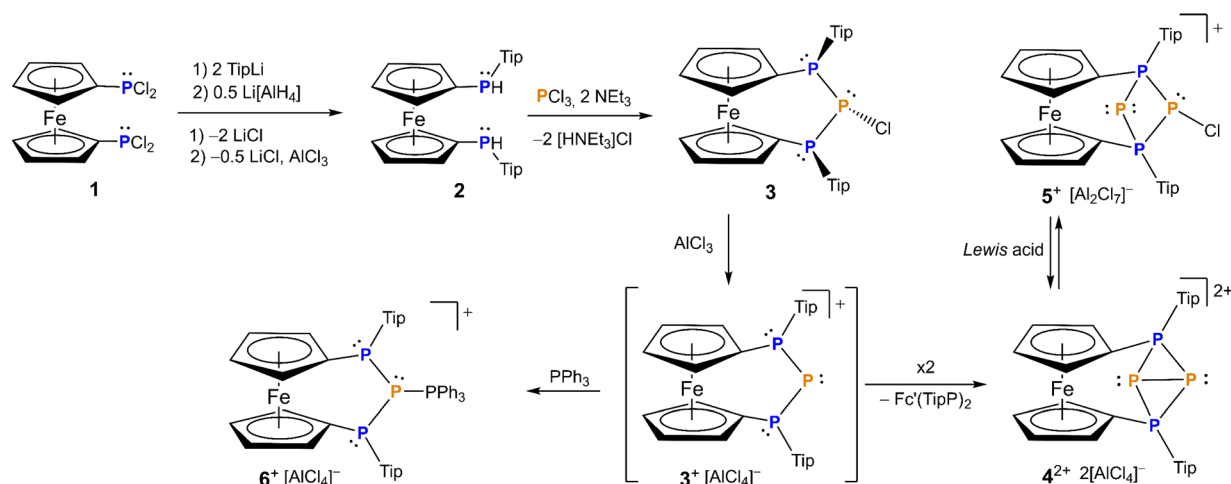
Results and discussion

As a starting point, we introduced 2,4,6-tri(isopropyl)phenyl (Tip) as a so far unexplored substituent at the phosphorus atoms of the [3]ferrocenophane scaffold following a previous established substitution and condensation sequence (Scheme 1).⁶⁴ We anticipated that the increased steric congestion would supply sufficient steric protection to prevent dimerization observed for the ^tBu substituted heterocarbenes.^{54,65}

To this end 1,1-bis(dichlorophosphanyl)ferrocene⁶⁶ is reacted with two equivalents of 2,4,6-tri(isopropyl)phenyl lithium (Tip–Li) then the resulting chlorophosphane is transformed

into the secondary hydrophosphane **2** which subsequently condenses with PCl₃ in the presence of base to form [3]ferrocenophane **3** (Scheme 1). Given the stereogenic nature of the phosphorus atoms in the terminal positions, it should be mentioned that prior to the ring closure the ferrocenophane precursor is a mixture of the corresponding *rac* and *meso* diastereomers of **2** for which *rac* **2** epimerizes upon reaction to **3**. The ferrocene bridged triphosphanyl scaffold limits the number of diastereomers originating from the presence of the *P*-stereogenic centers.⁶⁴ Interestingly, for Tip-substituted **3** exclusive formation of the *meso-trans*-isomer is observed, where *trans* refers to the orientation of the chlorine with respect to the Tip substituents. The computed Gibbs free energy difference between the *cis* and its corresponding *trans* isomer is small ($\Delta G = 2.9 \text{ kcal mol}^{-1}$ see Computational details in ESI†), comparable to the value obtained in case of the ^tBu-substituted counterpart, where both isomers were observed.⁶⁴ Assuming that interconversion of the isomers is unlikely due to the high inversion barrier of the phosphorus centers, the selective formation of the *trans* isomer of **3** can be attributed to kinetic factors rather than to its thermodynamic stability.

The ³¹P NMR spectrum of [3]ferrocenophane **3** features an AX₂ spin system, with the signal of the central phosphorus atom ($\delta(^{31}\text{P}) = 91.2 \text{ ppm}$) split into a triplet, whereas the two outer phosphorus nuclei resonating at -28.1 ppm feature a doublet splitting. The low ¹J_{PP} coupling constant of 177 Hz in **3** is in agreement with the formation of the *meso-trans* diastereomer since significantly higher values (*ca.* 350 Hz) are generally observed for *meso-cis*-triphospha[3]ferrocenophanes.⁶⁴ Although we were able to grow small orange crystals of **3**, these were not suitable for X-ray crystallography owing to extremely poor scattering. The identity and purity of **3** were further confirmed by ¹H, ¹³C-NMR spectroscopy and elemental analysis. The ³¹P resonances of both diastereomers of **2** are located at -97.9 ppm (as two overlapping resonances) featuring ¹J_{PH}-coupling of 226 Hz. Identity and purity of **2** were further confirmed by ¹H, ¹³C-NMR spectroscopy, mass spectrometry,



Scheme 1 Synthetic pathway to phosphonium ion **3**[AlCl₄], stabilized phosphonium ion **6**[AlCl₄] and tetraphosphonium ion **4**[AlCl₄]₂ with rearrangement to triphosphonium ion **5**[Al₂Cl₇].



elemental analysis and X-ray crystallography (Fig. S1†). The latter findings support significant steric congestion, with the angular sum at the phosphorus atoms ($\sum P1 = 332(4)^\circ$ and $\sum P2 = 325(3)^\circ$) in **2** being remarkably high and comparable to extremely bulky triarylphosphanes such as $P(\text{Mes})_3$ (330°)⁶⁷ or $P(\text{Tip})_3$ (337°).⁶⁷

With chlorophosphane **3** in hand, we set out to investigate chloride abstraction to the respective phosphonium ion. While with GaCl_3 or $\text{Li}[\text{Al}(\text{OC}(\text{CF}_3)_3)_4]$ no selective reactivity was found, for AlCl_3 complete and selective P^+ transfer to dicationic 4^{2+} and diphosphane $\text{Fc}(\text{TipP})_2$ was observed (Scheme 1). As intended the bulky Tip substituents successfully prevent dimerization of 3^+ , which had been observed for its ^tBu substituted analog IV^+ (Fig. 1).⁵⁴ However, stabilization of the flanking phosphanyl units is insufficient to isolate the free phosphonium ion 3^+ ,⁶⁸ resulting in formal elimination of “ P^+ ” which is transferred to a second unit of transient phosphonium cation 3^+ forming the thermodynamically more stable dication 4^{2+} . This hypothesis is thermodynamically plausible, as confirmed by the exergonic computed reaction Gibbs free energy for the “ P^+ ” transfer to cation 3^+ ($\Delta G = -5.1 \text{ kcal mol}^{-1}$, Computational details in ESI†). At this point, it is important to highlight that the formation of the corresponding bisphosphanylphosphonium dimer (analogue of $(IV^+)_2$) is thermodynamically favored ($\Delta G = -12.5 \text{ kcal mol}^{-1}$) over the formation of 4^{2+} ($\Delta G = -5.1 \text{ kcal mol}^{-1}$). The exergonic dimerization process, even in the presence of bulky groups, indicates the outstanding stability of this dimeric structural motif^{54,69,70} and implies that the formation of 4^{2+} is under kinetic control (proposed mechanism in Scheme S1 in the ESI†). Again, ^{31}P NMR spectra are helpful to establish the connectivity in 4^{2+} featuring two triplet resonances centered at $\delta = -213.9 \text{ ppm}$ (central phosphanyl units) and $\delta = 24.0 \text{ ppm}$ (tetra-coordinated phosphorus atoms) with a $^1J_{\text{PP}}$ coupling constant of 304 Hz, which is consistent with a rigid tetraphosphabicyclobutane. The identity and purity of $4[\text{AlCl}_4]_2$ was confirmed by ^1H , ^{13}C , ^{27}Al NMR spectroscopy and elemental analysis. The constitution of $4[\text{AlCl}_4]_2$ has been further corroborated by single crystal X-ray diffraction (Fig. 2).

The bisphosphonium ion 4^{2+} crystallizes without direct contact to its $[\text{AlCl}_4]^-$ counter anions and with almost plane-parallel arrangement of the Cp ligands ($\alpha = 2.7(2)^\circ$) indicating an unstrained ferrocenophane structure. The molecular structure in the solid state of $4[\text{AlCl}_4]_2$ shows a P_4 fold angle of $72.1(2)^\circ$, which is usually found for strongly puckered P_4 rings in diaryltetraphosphabicyclobutanes.^{71–73} In line with this a strongly distorted trigonal pyramidal geometry is found at P2 and P3 with an angular sum of $\sum P2 = 200.2(5)^\circ$ and $\sum P3 = 202.5(5)^\circ$. The P–P bond lengths [2.184(5) Å (P1–P2) and 2.171(5) Å (P1–P3)] between the tetrasubstituted outer and trisubstituted central phosphorus atoms are in the range of common P–P single bonds. Interestingly the bond between the two central phosphorus atoms is significantly elongated [2.335(5) Å P2–P3]. To the best of our knowledge, the tetraphosphonium salt $4[\text{AlCl}_4]_2$ contains the longest documented P–P single bond between two tricoordinated phosphorus atoms in a functionalized “ P_4 ”. Closely related to 4^{2+} are P_4 -adducts with cations such as Ag^+ , NO^+ , or PPh_2^+ reported by Krossing, Weigand and Riedel or the edge protonated $P_4\text{H}^+$ reported by Müller and Riedel.^{57,74–77}

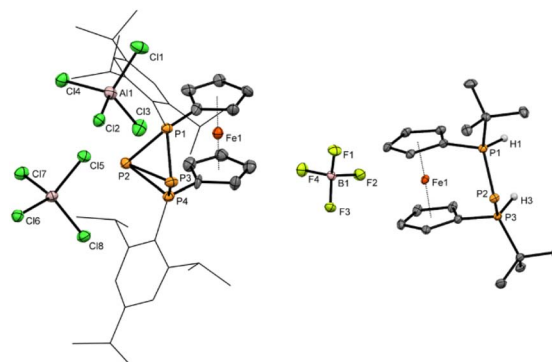


Fig. 2 Molecular structures of $4[\text{AlCl}_4]_2$ and $8c[\text{BF}_4]$ in the solid state. Ellipsoids are shown at 30% probability. All hydrogen atoms except H1 and H3, which are bonded to phosphorus atoms are omitted for clarity. The Tip substituents at P1 and P4 in $4[\text{AlCl}_4]_2$ are shown as wireframe. Selected bond lengths and angles in $4[\text{AlCl}_4]_2$: P1–P2 2.184(5) Å, P1–P3 2.171(5) Å, P2–P3 2.335(5) Å, P2–P4 2.194(5) Å, P3–P4 2.173(5) Å; $8c[\text{BF}_4]$: P1–P2 2.1284(7) Å, P2–P3 2.1265(7) Å, P1–H1 1.28(2) Å, P2–H2 1.26(2) Å, PPP-angle $89.50(2)^\circ$.

The bonding situation of 4^{2+} was explored by DFT calculations. Topological analysis was performed by the means of Bader's atoms in molecules (AIM) theory, and a bond critical point with electron density of 0.092 au was found between P2 and P3. In agreement with the shorter bond length, the electron density is higher (0.122 a.u.) in the bond critical points between atoms P1 and P2 (or P1 and P3). By examining the dimensionless ratios defined by Bader⁷⁸ and Espinosa⁷⁹ and other computed parameters, the interaction can be classified as a covalent bond (Tables S2–S5†). The Laplacian of the electron density along the P2–P3 bond path ($\nabla^2(r)$ function) shows a high degree of symmetry, with a local maximum of -0.0314 au at the bond critical point (see Fig. S2†). The rather weak character of the P2–P3 bond is reflected by the computed quantum theory of atoms in molecules (QTAIM) data, Mayer bond, and delocalization indices (see Tables S2–S4 in the ESI†) and the gradient plot of the Laplacian plot (see Fig. S3 and S4 in the ESI†). Natural resonance theory analysis proposes only one leading resonance structure for tetraphosphonium ion 4^{2+} with 70% weight, which is represented by the Lewis structure depicted in Scheme 1 and in Fig. 4 (structure D) (more details in the ESI†).

The analysis of Kohn–Sham orbitals shows that all four phosphorus atoms make significant contributions to the unoccupied orbitals (Fig. 3). The LUMO is basically the combination of the empty p_z orbitals at the central phosphorus atoms and the antibonding σ^* of the P2–P3 bond, which fore-shadows the reactivity of the central phosphorus atoms towards nucleophiles. The orbital-weighted Fukui function (which is a useful tool to identify the reactive site of a system)⁸⁰ verified the most electrophilic character of the central phosphorus atoms as well (Fig. S2 and S3 in the ESI†). The computed natural charge at each of the central phosphorus atoms is 0.21 which is in close agreement with the charges computed within QTAIM atomic basins. In view of these data, a possible alternative description of 4^{2+} could be a phosphonium ion intramolecularly stabilized by a triphosphonium ion (*cf.* C in Fig. 4), where the

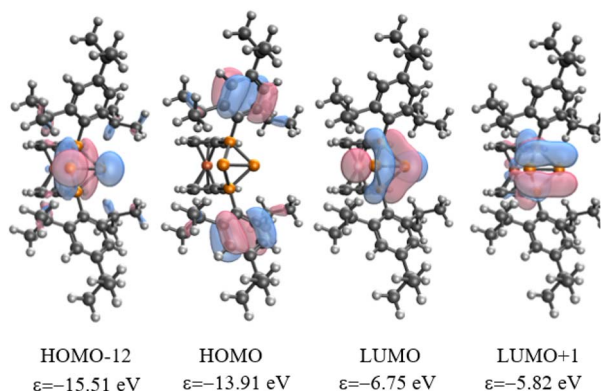


Fig. 3 Selected Kohn–Sham molecular orbitals of 4^{2+} at $\omega B97X-D/def2-TZVP$.

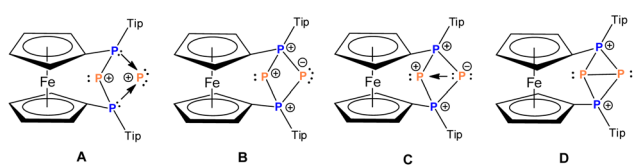


Fig. 4 Alternative Lewis-type descriptions of 4^{2+} .

triphosphenium part emerges from twofold coordination of P^+ by the phosphanyl groups of former 3^+ (cf. A and B in Fig. 4). However, the natural bond order in D, and QTAIM results indicate a purely covalent central P–P bond in line with the above-mentioned NRT results for 4^{2+} . Nonetheless, polar structures B or C, whilst not representative of the bonding situation, are useful to understand the reactivity of 4^{2+} (Schemes 1–3).

In order to evaluate the Lewis acid strength of 4^{2+} , its fluoride ion affinity (FIA) was computed (for single point energy calculations PCM = THF solvent model was applied), which is $87.2 \text{ kcal mol}^{-1}$. This value is significantly higher than the average of 27 dicationic compounds ($40.8 \text{ kcal mol}^{-1}$) recently investigated by Greb *et al.*⁸¹ and suggests super Lewis acidic character. (The corresponding vacuum phase FIA is $239.0 \text{ kcal mol}^{-1}$ for 4^{2+} and the average reported by Greb is $215 \text{ kcal mol}^{-1}$). In order to get a more precise picture (applying the same computational protocol) we have calculated phosphorus containing dicationic systems, where the positive charge is not localized at one center similar to 4^{2+} . Among the investigated cases (Table S6 in the ESI†) Dielmann's tricoordinate phosphorus dication $[P(\text{Nim})_3]^{2+}$ (im = 1,3-diisopropyl-4,5-dimethylimidazolin-2-yliden) exhibits a very similar FIA value

($87.9 \text{ kcal mol}^{-1}$), which was considered as Lewis superacid as well.⁸²

Tetraphosphenium salt $4[\text{AlCl}_4]_2$ is poorly soluble in halogenated solvents like chloroform, dichloromethane or 1,2-difluorobenzene. Isolated $4[\text{AlCl}_4]_2$ can be stored as solid under inert atmosphere for several weeks without decomposition but has a limited lifetime in solution. In solution, $4[\text{AlCl}_4]_2$ transforms quantitatively within several hours to a new product, which could be assigned to its chloride adduct $5[\text{Al}_2\text{Cl}_7]$ representing the first bicyclic triphosphenium ion (Scheme 1). The calculated reaction Gibbs free energy of the process is only $-0.1 \text{ kcal mol}^{-1}$. Since the small negative ΔG value does not exclude the reversibility of the process, the quantitative back-reaction to tetraphosphenium ion 4^{2+} was tested and after the addition of further Lewis acid (AlCl_3 or $\text{Li}[\text{Al}(\text{OC}(\text{CF}_3)_3)_4]$) 4^{2+} was detected. The mono cation $5[\text{Al}_2\text{Cl}_7]$ shows characteristic signals in the ^{31}P NMR spectrum (Table 1).

Thus, the resonance of the two chemically equivalent terminal phosphorus atoms at 19.5 ppm splits into a doublet of doublets owing to coupling with the central phosphanide center ($^1J_{\text{PP}} = 372 \text{ Hz}$) and the central P–Cl unit ($^1J_{\text{PP}} = 337 \text{ Hz}$). The same couplings are found for the signals of the central disubstituted phosphorus atom resonating at -130.7 ppm ($^1J_{\text{PP}} = 372 \text{ Hz}$, $^2J_{\text{PP}} = 108 \text{ Hz}$) and the chlorine substituted phosphorus atom at -39.8 ppm ($^1J_{\text{PP}} = 337 \text{ Hz}$, $^2J_{\text{PP}} = 108 \text{ Hz}$) which in turn split into doublets of triplets. The identity and purity of $5[\text{Al}_2\text{Cl}_7]$ was further confirmed by ^1H , ^{13}C NMR spectroscopy and elemental analysis. Since initially formed 3^+ was not directly observed spectroscopically, the formation of 3^+ as an intermediate was verified by trapping the phosphonium ion with the established Lewis base PPh_3 , leading to the formation of the expected triphenylphosphane-stabilized phosphonium ion **6** $[\text{AlCl}_4]$ (Scheme 1). Interestingly, **6**⁺ exhibits higher stability by $15.0 \text{ kcal mol}^{-1}$ (Scheme S2 in ESI†), than its *t*-Bu substituted counterpart.⁵⁴ The PPh_3 -adduct **6** $[\text{AlCl}_4]$ shows three different resonances in the ^{31}P NMR spectra with expected splitting patterns similar to a triphenylphosphane-stabilized phosphonium ion reported only recently.⁵⁴ The two chemically equivalent outer phosphorus nuclei show a resonance at 43.2 ppm, split into a doublet of doublets due to the coupling to the central phosphorus atom ($^1J_{\text{PP}} = 174 \text{ Hz}$) and the PPh_3 group ($^2J_{\text{PP}} = 72 \text{ Hz}$). The signal of the central phosphorus atom resonates at 5.2 ppm and splits into a doublet of triplets owing to coupling with the two chemically equivalent outer phosphanyl groups and the PPh_3 fragment ($^1J_{\text{PP}} = 379 \text{ Hz}$). The signal of the PPh_3 group in **6** $[\text{AlCl}_4]$ is found at 22.3 ppm with the expected doublet of triplet pattern resulting from the P–P couplings described above. Identity and purity of **6** $[\text{AlCl}_4]$ was

Table 1 Summary of ^{31}P NMR data of compounds **3–6** and **8c** (without consideration of ^1H – ^{31}P coupling)

Compound	$\delta(^{31}\text{P})$ [ppm]	$ J_{\text{PP}} $ [Hz]	Spin system
3	91.2(t), -28.1 (d)	177 ($^1J_{\text{AX}}$)	AX_2
4	24.0(t), -213.9 (t)	304 ($^1J_{\text{AX}}$)	A_2X_2
5	19.5(dd), -39.8 (dt), -130.7 (td)	372 ($^1J_{\text{AX}}$), 337 ($^1J_{\text{MX}}$), 108 ($^2J_{\text{AM}}$)	AMX_2
6	43.2(dd), 22.3(dt), 5.2(dt)	174 ($^1J_{\text{AX}}$), 72 ($^2J_{\text{MX}}$), 379 ($^1J_{\text{AM}}$)	AMX_2

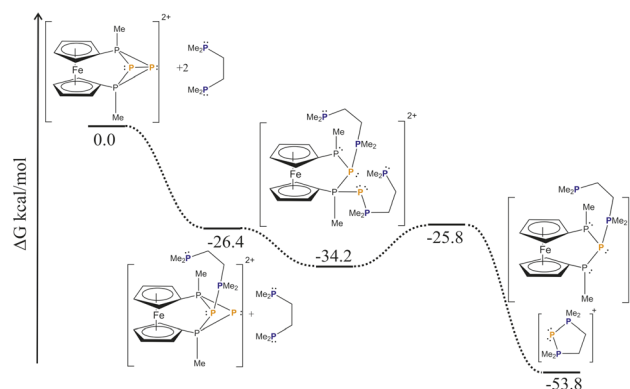


further confirmed by ^1H , ^{13}C , ^{27}Al NMR spectroscopy and elemental analysis.

The bonding situation along with the exceptionally long P–P bond in $4[\text{AlCl}_4]_2$ sparked us to explore the reactivity of this unprecedented species. Since 4^{2+} originates from P^+ transfer itself and its formation was not highly exergonic ($\Delta G = -5.1 \text{ kcal mol}^{-1}$), we were wondering whether this P^+ fragment may be further transferred to other substrates. Thus, we reacted $4[\text{AlCl}_4]_2$ with different bisphosphanes such as dppe (1,2-bis(diphenylphosphino)ethane), dppf (1,1'-bis(diphenylphosphino)ferrocene) and prochiral 1,1'-bis(*tert*-butylphosphino)ferrocene **7**. In all cases a formal P^+ transfer was obtained leading to selective formation of the corresponding triphosphenium ions **8a–c** (Scheme 2). As a by-product, the corresponding phosphonium cations stabilized by a second equivalent of bisphosphane were observed.

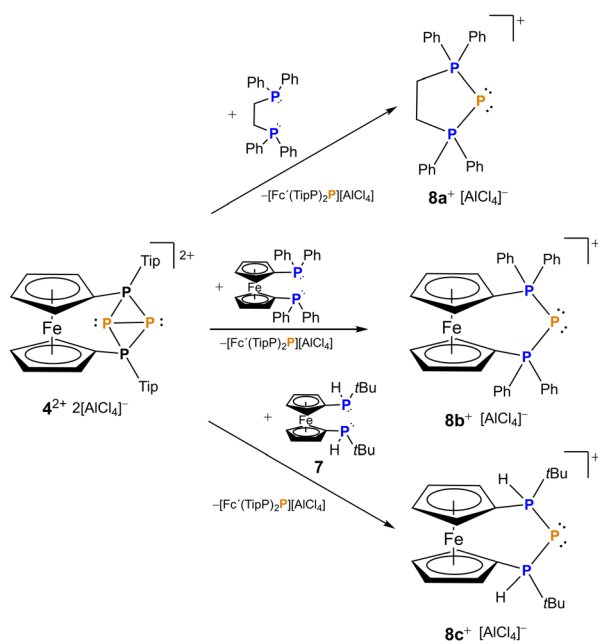
Our DFT calculations (Scheme 3, a model system with Me substituents at the phosphorus atoms was used, $\omega\text{B97X-D/def2-SVP}$) reveal that the nucleophilic attack of the bisphosphane to one of the central phosphorus atoms (P2) is a barrierless process, resulting in the cleavage of the central P2–P3 bond. The addition of a second bisphosphane to the other central phosphorus atom (P3) leads to the breakage of the bond between the central and the outer phosphorus atoms (P1–P3) and similar to the first addition it proceeds without any significant barrier. In the next step, the P3–P4 bond cleaves, and at the same time, the second phosphane unit of the bisphosphane closes the ring with the originally P3 phosphorus atom. The overall process has a significant thermodynamic driving force ($-53.8 \text{ kcal mol}^{-1}$).

While triphosphenium ions **8a,b** are already known in the literature and their successful formation was verified by ^{31}P -NMR spectroscopy,^{83,84} **8c** represents the first triphosphenium

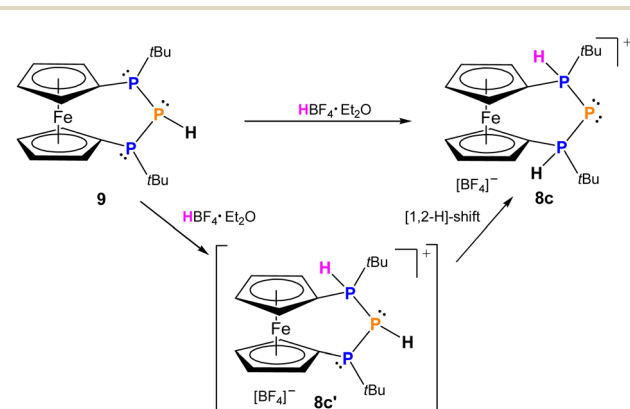


Scheme 3 Calculated reaction mechanism of the P^+ transfer reaction.

ion carrying hydrogen substituents at both phosphonium centers, in addition to one *tert*-butyl group. Given the unique possibilities of attaching or abstracting protic hydrogen atoms we explored an alternative access to **8c** starting from literature known **9**. The calculated proton affinity of **9** is $270.7 \text{ kcal mol}^{-1}$, and we found that HBF_4 is able to protonate secondary triphosphane **9** inducing a [1,2-H] shift of the proton already present at the central phosphorus atom resulting in selective formation of **8c** (Scheme 4), which is more stable by $1.9 \text{ kcal mol}^{-1}$, than the originally formed intermediate (**8c'**). Despite its simplicity this straightforward approach to triphosphenium ions *via* protonation of a secondary triphosphane is unprecedented in the current literature. A clear advantage over previously published protocols emerges from the selectivity of the reaction, as no byproducts are formed and **8c** can be isolated in good yields (65%) after first recrystallization. Regardless of whether **8c** is formed *via* a formal “ P^+ ” transfer to bisphosphane **7** or protonation of triphospha[3]ferrocenophane **9** the formation proceeds stereoselectively and **8c** is obtained in the *meso* form only, while there is no evidence for the appearance of its *rac* diastereomer neither in solution nor in solid state. In the ^{31}P -NMR spectra, protonation of the outer phosphorus atoms entails a significant downfield shift of these nuclei by more than 50 ppm resulting in a chemical shift at 42.5 ppm in **8c**. In turn,



Scheme 2 Synthesis of triphosphenium ions **8a–c** *via* formal P^+ transfer using $4[\text{AlCl}_4]_2$ starting from the corresponding bisphosphane.



Scheme 4 Synthesis of triphosphenium ion **8c** *via* protonation of triphosphane **9** with HBF_4 .



the central phosphorus atom encounters a drastic high field shift and resonates at -195.2 ppm in **8c** and the AX_2 spin system features a $^1J_{PP}$ -coupling constant of 456 Hz. These values are fully consistent with those of literature known triphosphenium ions reported by Schmidpeter or Macdonald.^{16,26,83,85} In addition the signal of the two outer phosphorus atoms in **8c** splits into a doublet with a $^1J_{PH}$ coupling constant of 468 Hz, which is typical for proton substituted phosphonium ions, as is the $\delta(^1H) = 7.07$ ppm. The identity and purity of isolated **8c** was further corroborated by 1H -, ^{11}B -, ^{13}C -, ^{19}F -NMR, mass spectrometry and elemental analysis.

In the solid state the *meso* arrangement in **8c** was confirmed by single crystal X-ray diffraction (Fig. 2). The ferrocenophane based triphosphenium ion **8c** crystallizes in an almost eclipsed conformation of the ferrocene unit ($\tau = 4.58(8)^\circ$) and plane-parallel arrangement of the Cp rings ($\alpha = 1.24(8)^\circ$). For the central phosphorus atom P2 of the P_3 -bridge, symmetric contacts to the adjacent phosphonium centers P1 (2.1284(7) Å (P1–P2)) and P3 (2.1265(7) Å (P2–P3)) are found. The P–P bond lengths in **8c** are somewhat shorter compared with other phosphorus-rich ferrocenophanes,^{54,64,65} indicative for delocalization of the negative charge across the *ansa*-bridge comparable to other cyclic triphosphenium ions.^{24,26,27} **8c** was investigated computationally to get further insight into its bonding situation. As expected, the HOMO is localized mainly (72%) at the central phosphorus and polarized towards the two outer phosphorus atoms, similar to other triphosphenium systems (Fig. S7 in the ESI†). In agreement with the shorter P–P bond lengths second order perturbation analysis on NBO basis revealed backdonation (~ 60 kcal mol $^{-1}$) from the central phosphorus atom (Table S7 in the ESI†).

Conclusion

To conclude, we demonstrated P^+ transfer from and to a transient phosphonium ion. The dication 4^{2+} resulting from P^+ addition to this phosphonium ion is stable and its salt $4[AlCl_4]_2$ is storable in the solid state for prolonged time. The latter serves as P^+ source itself and transforms various bisphosphanes to the corresponding triphosphenium ions, which was demonstrated for known as well as for unprecedented examples. In this context the first triphosphenium ion bearing hydrogen substituents at both phosphonium centers was obtained and a new synthetic pathway was demonstrated *via* simple protonation of a secondary triphosphane. In analogy to the existing class of triphosphenium ions we suggest the name tetraphosphenium ion for species 4^{2+} . The latter features the longest structurally characterized P–P bond involving tricoordinate phosphorus atoms reported so far. Moreover, its FIA value suggests Lewis superacidic character. Based on these new insights we aim at transferring P^+ ions to other cationic or electron deficient molecules and element fragments in future investigations. In terms of bonding situation, the here presented tetraphosphenium dication 4^{2+} is featuring a non-polar central P–P bond, whereas its reactivity (Schemes 1 and 3) involves heterolytic cleavage of the same bond with an alternative description assuming a polar nature of the electron

configurations (sextet and octet) at the central phosphorus atoms in 4^{2+} (cf. C, Fig. 4). It is well established, that closed-shell divalent phosphorus compounds (*i.e.* PR_2^+ and PR_2^-) may be regarded as a continuum of species, where depending on the electronic properties of the substituents R the reactivity ranges from nucleophilic to electrophilic.^{86,87} In this picture, the substituents R would be the phosphonio groups of 4^{2+} , concurrently allowing configurations with opposite polarity at the adjacent phosphorus atoms.

Data availability

The datasets supporting this article have been uploaded as part of the ESI.† Crystallographic data for **2**, **4** $[AlCl_4]_2$ and **8c** $[BF_4]$ have been deposited at the CCDC under 2328571–2328573 and can be obtained from <https://www.ccdc.cam.ac.uk/structures>.

Author contributions

The manuscript was written through contributions of all authors. All authors have given approval to the final version of the manuscript.

Conflicts of interest

There are no conflicts to declare.

Acknowledgements

The authors would like to acknowledge funding by the Deutsche Forschungsgemeinschaft (DFG, German Research Foundation) – Projektnummer 328961117 – SFB 1319 ELCH. ZK is grateful for the general support of János Bolyai Research Scholarship and OTKA (FK-145841) provided by the Hungarian National Research Development and Innovation Office.

References

- 1 D. Heift, Z. Benkő, H. Grützmacher, A. R. Jupp and J. M. Goicoechea, *Chem. Sci.*, 2015, **6**, 4017–4024.
- 2 T. P. Robinson, M. J. Cowley, D. Scheschkewitz and J. M. Goicoechea, *Angew. Chem., Int. Ed.*, 2015, **54**, 683–686.
- 3 L. N. Grant, B. Pinter, B. C. Manor, R. Suter, H. Grützmacher and D. J. Mindiola, *Chem.–Eur. J.*, 2017, **23**, 6272–6276.
- 4 M. Joost, W. J. Transue and C. C. Cummins, *Chem. Commun.*, 2017, **53**, 10731–10733.
- 5 G. Hierlmeier, A. Hinz, R. Wolf and J. M. Goicoechea, *Angew. Chem., Int. Ed.*, 2018, **57**, 431–436.
- 6 A. Hinz and J. M. Goicoechea, *Dalton Trans.*, 2018, **47**, 8879–8883.
- 7 A. Hinz and J. M. Goicoechea, *Chem.–Eur. J.*, 2018, **24**, 7358–7363.
- 8 J. Abbenseth, M. Diefenbach, A. Hinz, L. Alig, C. Würtele, J. M. Goicoechea, M. C. Holthausen and S. Schneider, *Angew. Chem., Int. Ed.*, 2019, **58**, 10966–10970.
- 9 Y. Wang, T. Szilvási, S. Yao and M. Driess, *Nat. Chem.*, 2020, **801**–807.



- 10 S. Bestgen, M. Mehta, T. C. Johnstone, P. W. Roesky and J. M. Goicoechea, *Chem.-Eur. J.*, 2020, **26**, 9024–9031.
- 11 A. Reinholdt, M. G. Jafari, C. Sandoval-Pauker, E. Ballester-Martínez, M. R. Gau, M. Driess, B. Pinter and D. J. Mindiola, *Angew. Chem., Int. Ed.*, 2021, **60**, 17595–17600.
- 12 M. G. Jafari, Y. Park, B. Pudasaini, T. Kurogi, P. J. Carroll, D. M. Kaphan, J. Kropf, M. Delferro, M.-H. Baik and D. J. Mindiola, *Angew. Chem., Int. Ed.*, 2021, **60**, 24411–24417.
- 13 B. L. Frenette, J. Trach, M. J. Ferguson and E. Rivard, *Angew. Chem., Int. Ed.*, 2023, **62**, e202218587.
- 14 J. M. Goicoechea and H. Grützmacher, *Angew. Chem., Int. Ed.*, 2018, **57**, 16968–16994.
- 15 J. H. W. LaFortune, A. Swidan, J. S. Ovens, Z.-W. Qu, S. Grimme, M. A. Land and C. L. B. Macdonald, *Chem.-Eur. J.*, 2023, **29**, e202302558.
- 16 E. M. Dionisi, J. F. Binder, J. H. W. LaFortune and C. L. B. Macdonald, *Dalton Trans.*, 2020, **49**, 12115–12127.
- 17 J. F. Binder, A. Swidan and C. L. B. Macdonald, *Inorg. Chem.*, 2018, **57**, 11717–11725.
- 18 S. C. Kosnik, M. C. Nascimento, J. F. Binder and C. L. B. Macdonald, *Dalton Trans.*, 2017, **46**, 17080–17092.
- 19 C. L. B. Macdonald, J. F. Binder, A. Swidan, J. H. Nguyen, S. C. Kosnik and B. D. Ellis, *Inorg. Chem.*, 2016, **55**, 7152–7166.
- 20 S. C. Kosnik and C. L. B. Macdonald, *Dalton Trans.*, 2016, **45**, 6251–6258.
- 21 F. O. Elnajjar, J. F. Binder, S. C. Kosnik and C. L. B. Macdonald, *Z. Anorg. Allg. Chem.*, 2016, **642**, 1251–1258.
- 22 J. F. Binder, A. Swidan, M. Tang, J. H. Nguyen and C. L. B. Macdonald, *Chem. Commun.*, 2015, **51**, 7741–7744.
- 23 B. D. Ellis, C. A. Dyker, A. Decken and C. L. B. Macdonald, *Chem. Commun.*, 2005, **15**, 1965–1967.
- 24 J. W. Dube, C. L. B. Macdonald and P. J. Ragogna, *Angew. Chem., Int. Ed.*, 2012, **51**, 13026–13030.
- 25 A. Schmidpeter, S. Lochschmidt and W. S. Sheldrick, *Angew. Chem., Int. Ed.*, 1982, **21**, 63–64.
- 26 A. Schmidpeter, S. Lochschmidt and W. S. Sheldrick, *Angew. Chem., Int. Ed.*, 1985, **24**, 226–227.
- 27 E. L. Norton, K. L. S. Szekely, J. W. Dube, P. G. Bomben and C. L. B. Macdonald, *Inorg. Chem.*, 2008, **47**, 1196–1203.
- 28 Y. Mizuhata, T. Sasamori and N. Tokitoh, *Chem. Rev.*, 2009, **109**, 3479–3511.
- 29 M. He, C. Hu, R. Wei, X.-F. Wang and L. L. Liu, *Chem. Soc. Rev.*, 2024, **53**, 3896–3951.
- 30 H. F. T. Klare, L. Albers, L. Süss, S. Keess, T. Müller and M. Oestreich, *Chem. Rev.*, 2021, **121**, 5889–5985.
- 31 S. Fleming, M. K. Lupton and K. Jekot, *Inorg. Chem.*, 1972, **11**, 2534–2540.
- 32 B. E. Maryanoff and R. O. Hutchins, *J. Org. Chem.*, 1972, **37**, 3475–3480.
- 33 D. Gudat, in *Comprehensive Inorganic Chemistry II*, eds. J. Reedijk and K. Poeppelmeier, Elsevier, Amsterdam, 2nd edn, 2013, pp. 587–621.
- 34 A. H. Cowley and R. A. Kemp, *Chem. Rev.*, 1985, **85**, 367–382.
- 35 N. Burford, B. W. Royan, A. Linden and T. S. Cameron, *J. Chem. Soc., Chem. Commun.*, 1988, 842–844.
- 36 N. Burford, T. S. Cameron, P. J. Ragogna, E. Ocampo-Mavarez, M. Gee, R. McDonald and R. E. Wasylshen, *J. Am. Chem. Soc.*, 2001, **123**, 7947–7948.
- 37 N. Burford, P. J. Ragogna, R. McDonald and M. J. Ferguson, *J. Am. Chem. Soc.*, 2003, **125**, 14404–14410.
- 38 R. Pietschnig, *J. Organomet. Chem.*, 2007, **692**, 3363–3369.
- 39 Y.-y. Carpenter, C. A. Dyker, N. Burford, M. D. Lumsden and A. Decken, *J. Am. Chem. Soc.*, 2008, **130**, 15732–15741.
- 40 S. Weller, S. H. Schlindwein, C. M. Feil, Z. Kelemen, D. Buzsáki, L. Nyulászi, S. Isenberg, R. Pietschnig, M. Nieger and D. Gudat, *Organometallics*, 2019, **38**, 4717–4725.
- 41 J. M. Slattery and S. Hussein, *Dalton Trans.*, 2012, **41**, 1808–1815.
- 42 T. Zhang, V. Y. Lee, S. Morisako, S. Aoyagi and T. Sasamori, *Eur. J. Inorg. Chem.*, 2021, **2021**, 3988–3991.
- 43 A. L. Brazeau, C. A. Caputo, C. D. Martin, N. D. Jones and P. J. Ragogna, *Dalton Trans.*, 2010, **39**, 11069–11073.
- 44 B. Rao, C. C. Chong and R. Kinjo, *J. Am. Chem. Soc.*, 2018, **140**, 652–656.
- 45 C. M. Feil, T. D. Hettich, K. Beyer, C. Sondermann, S. H. Schlindwein, M. Nieger and D. Gudat, *Inorg. Chem.*, 2019, **58**, 6517–6528.
- 46 M. Papendick and D. Gudat, *Chem.-Eur. J.*, 2023, **29**, e202302525.
- 47 A. Schmidpeter and M. Thiele, *Angew. Chem., Int. Ed.*, 1991, **30**, 308–310.
- 48 D. Gudat, M. Schrott and M. Nieger, *Chem. Commun.*, 1995, 1541–1542.
- 49 C. C. Chong, B. Rao, R. Ganguly, Y. Li and R. Kinjo, *Inorg. Chem.*, 2017, **56**, 8608–8614.
- 50 M. Olaru, A. Mischin, L. A. Malaspina, S. Mebs and J. Beckmann, *Angew. Chem., Int. Ed.*, 2020, **59**, 1581–1584.
- 51 S. G. Baxter, R. L. Collins, A. H. Cowley and S. F. Sena, *J. Am. Chem. Soc.*, 1981, **103**, 714–715.
- 52 A. Kraft, J. Beck and I. Krossing, *Chem.-Eur. J.*, 2011, **17**, 12975–12980.
- 53 M. Olaru, S. Mebs and J. Beckmann, *Angew. Chem., Int. Ed.*, 2021, **60**, 19133–19138.
- 54 R. Franz, B. Szathmári, C. Bruhn, Z. Kelemen and R. Pietschnig, *Inorg. Chem.*, 2023, **62**, 4341–4350.
- 55 C. Riesinger, A. Erhard and M. Scheer, *Chem. Commun.*, 2023, **59**, 10117–10120.
- 56 S. Reichl, E. Mädl, F. Riedlberger, M. Piesch, G. Balázs, M. Seidl and M. Scheer, *Nat. Commun.*, 2021, **12**, 5774.
- 57 J. J. Weigand, M. Holthausen and R. Fröhlich, *Angew. Chem., Int. Ed.*, 2009, **48**, 295–298.
- 58 D. Gudat, *Coord. Chem. Rev.*, 1997, **163**, 71–106.
- 59 M. Weber, G. Balázs, A. V. Virovets, E. Peresyphkina and M. Scheer, *Molecules*, 2021, **26**, 3920.
- 60 G. Balázs, A. Seitz and M. Scheer, in *Comprehensive Inorganic Chemistry II*, ed. J. Reedijk and K. Poeppelmeier, Elsevier, Amsterdam, 2nd edn, 2013, pp. 1105–1132.
- 61 A. H. Cowley, R. A. Kemp, J. G. Lasch, N. C. Norman and C. A. Stewart, *J. Am. Chem. Soc.*, 1983, **105**, 7444–7445.
- 62 K. Izod, P. Evans and P. G. Waddell, *Angew. Chem., Int. Ed.*, 2019, **58**, 11007–11012.



- 63 R. Franz, D. Gál, C. Bruhn, Z. Kelemen and R. Pietschnig, *Adv. Sci.*, 2024, **11**, 2306805.
- 64 S. Borucki, Z. Kelemen, M. Maurer, C. Bruhn, L. Nyulaszi and R. Pietschnig, *Chem.–Eur. J.*, 2017, **23**, 10438–10450.
- 65 S. Isenberg, S. Weller, D. Kargin, S. Valić, B. Schwederski, Z. Kelemen, C. Bruhn, K. Krekić, M. Maurer, C. M. Feil, M. Nieger, D. Gudat, L. Nyulászi and R. Pietschnig, *ChemistryOpen*, 2019, **8**, 1235–1243.
- 66 C. Moser, A. Orthaber, M. Nieger, F. Belaj and R. Pietschnig, *Dalton Trans.*, 2006, 3879–3885.
- 67 R. T. Boéré and Y. Zhang, *J. Organomet. Chem.*, 2005, **690**, 2651–2657.
- 68 D. Buzsáki, L. Nyulászi, R. Pietschnig, D. Gudat and Z. Kelemen, *Organometallics*, 2022, **41**, 2551–2561.
- 69 S. Nasemann, R. Franz, D. Kargin, C. Bruhn, Z. Kelemen, T. Gutmann and R. Pietschnig, *Chem.–Asian J.*, 2024, **19**, e202300950.
- 70 D. Kargin, Z. Kelemen, K. Krekić, L. Nyulászi and R. Pietschnig, *Chem.–Eur. J.*, 2018, **24**, 16774–16778.
- 71 A. R. Fox, R. J. Wright, E. Rivard and P. P. Power, *Angew. Chem., Int. Ed.*, 2005, **44**, 7729–7733.
- 72 R. J. Schwamm, M. Lein, M. P. Coles and C. M. Fitchett, *Angew. Chem., Int. Ed.*, 2016, **55**, 14798–14801.
- 73 J. Bresien, K. Faust, C. Hering-Junghans, J. Rothe, A. Schulz and A. Villinger, *Dalton Trans.*, 2016, **45**, 1998–2007.
- 74 A. Wiesner, S. Steinhauer, H. Beckers, C. Müller and S. Riedel, *Chem. Sci.*, 2018, **9**, 7169–7173.
- 75 K. F. Hoffmann, A. Wiesner, N. Subat, S. Steinhauer and S. Riedel, *Z. Anorg. Allg. Chem.*, 2018, **644**, 1344–1348.
- 76 T. Köchner, S. Riedel, A. J. Lehner, H. Scherer, I. Raabe, T. A. Engesser, F. W. Scholz, U. Gellrich, P. Eiden, R. A. Paz Schmidt, D. A. Plattner and I. Krossing, *Angew. Chem., Int. Ed.*, 2010, **49**, 8139–8143.
- 77 I. Krossing and L. van Wüllen, *Chem.–Eur. J.*, 2002, **8**, 700–711.
- 78 R. F. W. Bader and H. Essén, *J. Chem. Phys.*, 1984, **80**, 1943–1960.
- 79 E. Espinosa, I. Alkorta, J. Elguero and E. Molins, *J. Chem. Phys.*, 2002, **117**, 5529–5542.
- 80 R. Pino-Rios, O. Yañez, D. Inostroza, L. Ruiz, C. Cardenas, P. Fuentealba and W. Tiznado, *J. Comput. Chem.*, 2017, **38**, 481–488.
- 81 P. Erdmann, M. Schmitt, L. M. Sigmund, F. Krämer, F. Breher and L. Greb, *Angew. Chem., Int. Ed.*, 2024, **63**, e202403356.
- 82 P. Mehlmann, T. Witteler, L. F. B. Wilm and F. Dielmann, *Nat. Chem.*, 2019, **11**, 1139–1143.
- 83 S. Lochschmidt and A. Schmidpeter, *Z. Naturforsch. B*, 1985, **40**, 765–773.
- 84 J. D. Burton, R. M. K. Deng, K. B. Dillon, P. K. Monks and R. J. Olivey, *Heteroat. Chem.*, 2005, **16**, 447–452.
- 85 S. Kosnik, J. F. Binder, M. C. Nascimento and C. L. B. Macdonald, *J. Visualized Exp.*, 2016, e55021.
- 86 D. Gudat, *Coord. Chem. Rev.*, 1997, **163**, 71–106.
- 87 L. Rosenberg, *Coord. Chem. Rev.*, 2012, **256**, 606–626.

